

# Implementation and Evaluation of Four Wave Mixing in Optical Gyroscopes

A thesis submitted in partial fulfillment of the requirement  
for the degree of Bachelor of Science in Physics from  
The College of William and Mary

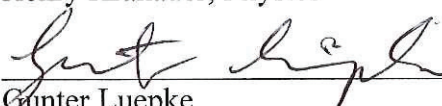
by

Jesse Evans

Accepted for Honors

  
Irina Nevikova, Director

  
Henry Krakauer, Physics

  
Gunter Luepke

Williamsburg, VA  
April 22, 2014

# Implementation and Evaluation of Four Wave Mixing in Optical Gyroscopes

Jesse Evans

*Adviser: Dr. Irina Novikova*

## Abstract

The purpose of the experiment was to build and test a 4 mirror laser cavity for the purpose of testing enhanced optical gyroscope capabilities. Probe, pump, and repump fields interacted with a Rubidium-87 cell inside the cavity for the purpose of enhanced measurement of rotational velocity through observation of changing cavity resonance frequencies. Interactions inside the cell produced slow and fast light in four wave mixing schemes in a four level N-scheme which theoretically cause resonance frequencies to shift farther for a given rate of cavity rotation, resulting in finer measurements of angular velocity. We were able to observe superluminal propagation and four wave mixing within the cavity setup, but have thus far been unable to observe enhanced gyroscopic properties.

# Contents

<b>1 Introduction</b>	<b>4</b>
<b>2 Theory</b>	<b>5</b>
<b>3 Experimental Overview</b>	<b>14</b>
<b>4 Experimental Details</b>	<b>16</b>
<b>5 Results and Analysis</b>	<b>25</b>
<b>6 Conclusions</b>	<b>31</b>
<b>7 Acknowledgements</b>	<b>32</b>
<b>8 References</b>	<b>33</b>

## Introduction

Optical gyroscopes are used in a wide variety of navigational systems. They precisely measure rotation in helicopters, aircraft, satellites, missiles, and unmanned drones without the use of GPS elements. A laser gyroscope consists of two counter-propagating light waves circulating inside an optical cavity. The light waves propagate in opposite directions inside the device and develop a phase difference according to the Sagnac Effect which is proportional to the rotational velocity of the cavity [2]. The resonant frequencies inside the device are shifted proportional to the rotation, providing a means of rotational velocity measurement based on measuring changes in resonant frequencies.

The hardware's measurement precision is crucial to its operation. We can gain more precision in optical gyroscope measurements by using fast light in conjunction with its normal operation. It has been proposed in recent studies that using these types of systems will allow for larger shifts in resonant frequencies given a rate of rotation, allowing for more precise measurement [1].

Our group has constructed a cavity that successfully optically resonates for given frequencies of a probe field. We have observed transmission within absorption lines of  $^{87}\text{Rb}$  through the phenomenon of Electromagnetically Induced Transmission (EIT) when we added a pump field. We then added a repump field and observed Four Wave Mixing (FWM) characterized by field generation. Finally, we observed the propagation of our probe field seeing both delay and advancement, which are characteristics of slow and fast light respectively.

# Theory

## Optical Cavities

Optical cavities work by having two or more mirrors aligned to continuously reflect a laser field internally, in a line in the case of a 2 mirror system or a triangle or square in the cases of a 3 or 4 mirror system (square cavity shown in figure 1).

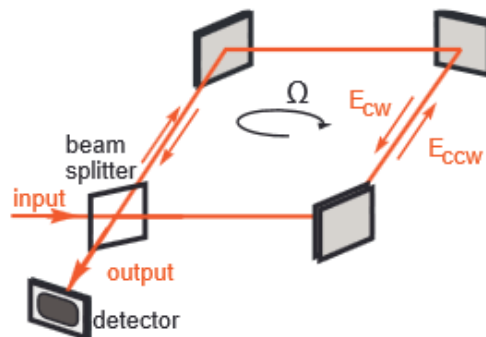


Figure 1 A four mirror cavity with optical fields [2]

When the cavity is in resonance, the laser is transmitted through mirrors after large numbers of internal reflections. A cavity is in resonance when the optical field within the cavity repeats itself each time around the cavity. The field meets this condition when

$$k = \frac{q\pi}{L}$$

where  $q$  is any integer,  $k$  is the wavevector, and  $L$  is the path length of the cavity. Given that

$$v = \frac{ck}{2\pi}$$

where  $v$  is the frequency and  $c$  is the speed of light, we can say that resonance frequencies for the cavity are

$$v_r = \frac{qc}{2L}$$

We can also see then that there is no single resonant frequency for a cavity, but infinitely many.

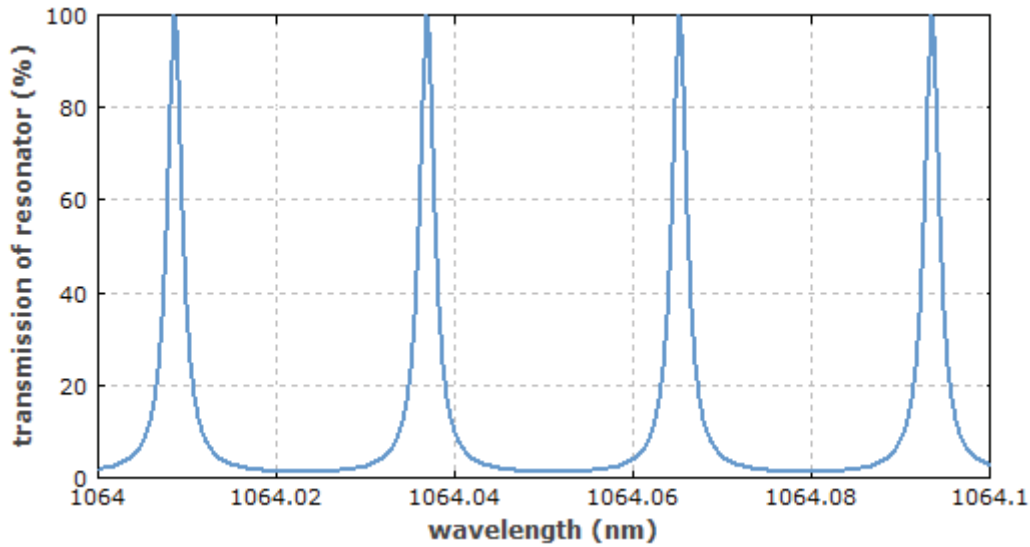


**Figure 2** Resonance frequency peaks  
from the RP Photonics Encyclopedia

The distance between two adjacent peaks in frequency space is known as the free spectral range (FSR), which is calculated theoretically as

$$\begin{aligned}
 FSR &= \nu_{r2} - \nu_{r1} = \frac{(q+1)c}{2L} - \frac{qc}{2L} \\
 &= \frac{c}{2L}
 \end{aligned}$$

The finesse of a cavity is an approximate value for how many trips around the cavity a photon will make inside the cavity. If the finesse of the cavity is low, high optical losses are expected.

$$\text{finesse} = \frac{FSR}{FWHM}$$

where FWHM is the full width at half max of the resonant peak.

It should also be noted that transverse cavity spatial modes need to be taken into account when dealing with laser cavities. Fields within a cavity must obey boundary conditions set

by the arrangements of the mirrors and other interactive elements inside the cavity. If a field's physical profile outside the cavity does not meet the boundary conditions inside the cavity, the field can excite undesirable higher order spatial modes. One can avoid undesirable modes by calculating the profile of the beam inside and outside the cavity and by using lenses and mirrors to cause the two profiles to match. In our experiment, the desired mode is TEM<sub>00</sub>, the transverse mode associated with a Gaussian intensity distribution given by

$$I(r, z) = I_0 \left( \frac{\omega_0}{\omega(z)} \right)^2 e^{\frac{-2r^2}{\omega(z)^2}}$$

where  $\omega_0$  is the beam's waist (its width at the narrowest point),  $\omega(z)$  is the beam's width at a given point on the z axis, and  $I_0$  is the beam's intensity at its narrowest point.

### *Optical Gyroscopes*

Optical gyroscopes operate via the Sagnac effect, whereby two laser fields are passed along the inside of an optical cavity in opposite directions. When the cavity is rotated, these two fields pick up a phase difference and their resonant frequencies shift. One can interpret this as the laser fields experiencing different path lengths, with the field in the direction of the rotation seeing that the path length is longer and the other that the path length is shorter. When the gyroscope is rotated, the two beams experience a time delay or advancement such that

$$t_{\pm} = \frac{2\pi R \pm \Delta L}{c}$$

where  $\Delta L$  is the change in path length the laser experiences, given by

$$\Delta L = R\omega t_{\pm}$$

which can be substituted into the equation for time delay to give

$$t_{\pm} = \frac{2\pi R}{c \pm R\omega}$$

and a difference in time experienced by

$$\Delta t = t_+ - t_- = \frac{4\pi R^2 \omega}{c^2 - R^2 \omega^2}$$

Substituting in for A, the area of a circle, and assuming that the rotation of the cavity is much less than the speed of light, we can then say

$$\Delta t = \frac{4A\omega}{c^2}$$

One can then recombine the fields outside the cavity and observe the resulting interference pattern to observe information about the phase difference. The shift in phase is given by

$$\Delta\phi = \frac{2\pi c \Delta t}{\lambda} = \frac{8\pi A\omega}{\lambda c}$$

where  $\lambda$  is the wavelength of light. The change in resonant frequency is given by

$$\Delta\nu = \frac{q c}{\Delta L}$$

Dividing  $\Delta\nu$  by  $\nu$  and accounting for a dispersive medium gives

$$\Delta\nu = \frac{\nu L}{n_g \Delta L} = \frac{\nu L}{n_g R \omega t_{\pm}}$$

where  $n_g$  is the group index of refraction and  $t_{\pm}$  is given above [2].

## *EIT*

Electromagnetically induced transmission is the phenomenon in which light is fully transmitted within an absorption line of an atomic medium. It occurs when the medium interacts with two fields of specific frequencies, a probe field and a control field. EIT begins with the treatment of a 3-level single  $\Lambda$  system with quantum states  $|1\rangle$ ,  $|2\rangle$ , and  $|3\rangle$  where

an electron can transition between the  $|1\rangle$  and  $|3\rangle$  and the  $|2\rangle$  and  $|3\rangle$  states according to selection rules (see figure 3).

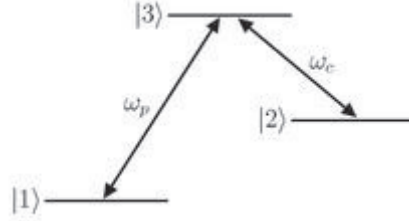


**Figure 3** Arbitrary 3 level single  $\Lambda$  system

The system has a wave equation given by

$$\psi = c_1(t)e^{-i\omega_1 t}|1\rangle + c_2(t)e^{-i\omega_2 t}|2\rangle + c_3(t)e^{-i\omega_3 t}|3\rangle$$

and can be operated upon by a Hamiltonian given by

$$H = H_0 + H_1$$

where

$$H_0 = \hbar\omega_1|1\rangle\langle 1| + \hbar\omega_2|2\rangle\langle 2| + \hbar\omega_3|3\rangle\langle 3|$$

$$H_1 = -\frac{\hbar}{2}(\Omega_p e^{-i\omega_p t}|1\rangle\langle 3| + \Omega_c e^{-i\omega_c t}|2\rangle\langle 3|)$$

where  $\Omega_p$  is the Rabi frequency corresponding to the probe field and  $\Omega_c$  is the Rabi frequency corresponding the control field.  $H_1$  is the portion of the Hamiltonian that is particularly relevant to our discussion, as it describes the transitions between states in the form of perturbation theory. After applying the Hamiltonian to the system and solving the Schrodinger equation,

$$H|\psi\rangle = i\hbar\frac{d}{dt}|\psi\rangle$$

which can be further solved such that there is a dark state that is only a linear combination of states  $|1\rangle$  and  $|2\rangle$  if the system is in what is known as the dark state:

$$|D\rangle = c_1(t)|1\rangle - c_2(t)|2\rangle$$

with coefficients given by

$$c_1(t) = \frac{\Omega_c}{\sqrt{\Omega_p + \Omega_c}}$$

$$c_2(t) = \frac{\Omega_p}{\sqrt{\Omega_p + \Omega_c}}$$

Note that the dark state contains no components of  $|3\rangle$ , which results in the lack of absorption within the medium at the given frequencies because transitions to the  $|3\rangle$  state are no longer allowed and thus energy cannot be absorbed from the photon. The dark state is stable and does not have a theoretical time dependence, although the state has a limited lifetime in experimental situations [7].

### *Four Wave Mixing*

In the four wave mixing process, 3 waves enter a medium, resulting in generation of another wave. When 3 fields are applied to the medium, the electric field entering the medium is given by

$$E(t) = E_1 e^{-i\omega_1 t} + E_2 e^{-i\omega_2 t} + E_3 e^{-i\omega_3 t}$$

and the nonlinear polarization of atoms is given by

$$P(t) = \chi E(t)^3$$

which results in many frequency components for the resultant wave polarization where  $\chi$  is the nonlinear electric susceptibility of the material. These frequency components can be tuned to produce a desired output by manipulating the intensity of the incoming waves [6].

In our experiment we input the probe and two control waves and generate light with frequency corresponding to the  $|4\rangle$  to  $|1\rangle$  and  $|3\rangle$  to  $|2\rangle$  transitions. Due to our experimental parameters, we do not see the  $|4\rangle$  to  $|1\rangle$  transition light, so our generation is all of the  $|3\rangle$  to  $|2\rangle$  variety, corresponding to the probe frequency.

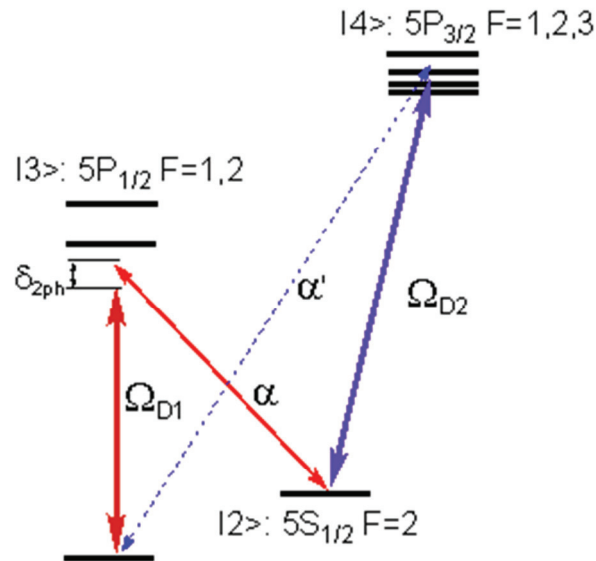


Figure 4 Four level N-scheme in  $^{87}\text{Rb}$

Our atomic system was in a 4 level Rubidium-87 N-scheme (figure 5).  $^{87}\text{Rb}$  has one valence electron that is in the ground state when it occupies one of the  $5S_{1/2}$  levels and in the excited state when it occupies one of the  $5P_{1/2}$  or  $5P_{3/2}$  levels. The transition to the  $5P_{1/2}$  is referred to as the D1 line of  $^{87}\text{Rb}$  and the transition to  $5P_{3/2}$  is referred to as the D2 line of  $^{87}\text{Rb}$ . In our experiment we tuned our lasers such that the probe field excited the  $F=2$  to  $F'=1$  or  $F'=2$  transition in the D1 line, the first control field (referred to the “pump” field for the rest of this paper) corresponds to the  $F=1$  to  $F'=1$  or  $F'=2$  transition in the D1 line, and the second control field (referred to as the “repump” field for the rest of this paper) is tuned to the  $F=2$  to  $F'=1, 2,$  or  $3$  transition in the D2 line.

### *Slow and Fast Light*

Slow light is the phenomenon where a pulse of light experiences a large refractive index and positive dispersion over a narrow bandwidth and thus slows down in a medium. The group velocity of a pulse of light is given by

$$v_g = \frac{c}{n_g}$$

where the group index

$$n_g = n_0 + \omega \frac{dn}{d\omega}$$

and  $n_0$  is the unmodified index of refraction and  $\omega$  is the frequency of light. Note that if  $\frac{dn}{d\omega}$  is non-zero, the group velocity can either increase or decrease. An increase in velocity yields fast light and a decrease yields slow light. Slow light is achieved in an EIT system (among other ways) through positive dispersion due to changes in the absorption. This was expressed in the 1920s through derivation of the Kramers Kronig relation for index of refraction [7][8]. Fast light is achieved (at least in our system) by adding another laser field that excites another transition in the medium, creating what is known as a double  $\Lambda$  system. This system is characterized by negative dispersion, and therefore the medium has a group index less than one when excited by the probe and two control fields (figure 45).

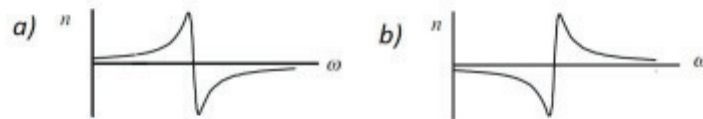


**Figure 5 a)** Steep negative dispersion in a fast light regime **b)** Positive dispersion in a slow light regime[4]

## Experimental Setup Overview

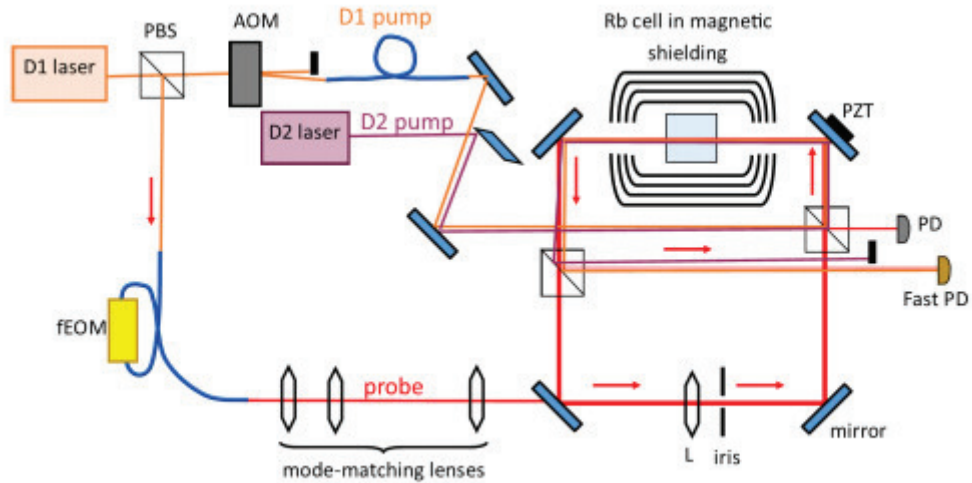


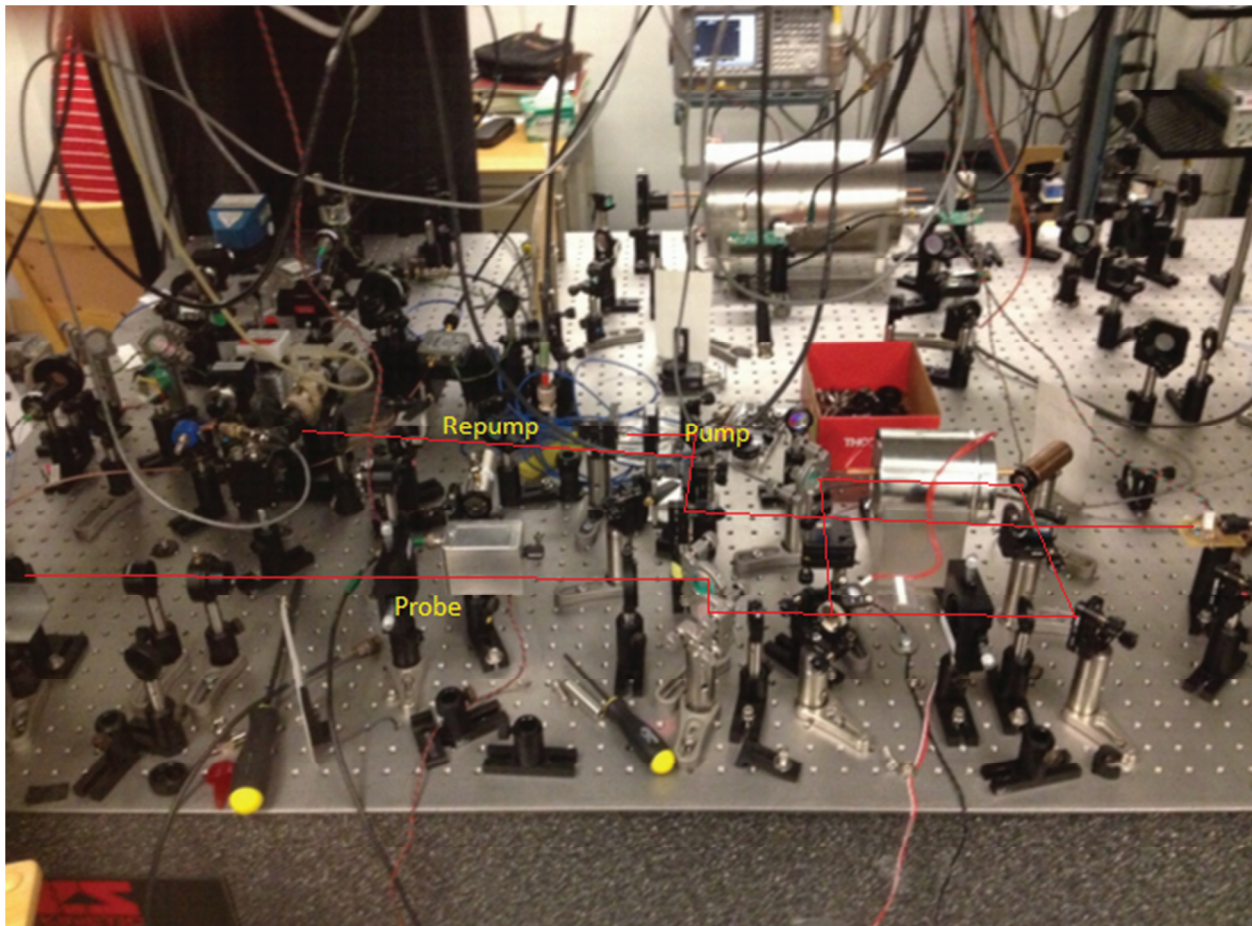
Figure 6 Design schematic of cavity setup

Figure 6 shows the experimental design represented symbolically and figure 7 shows a picture of the setup. A laser tuned to the D1 line of Rb is split by a polarizing beam splitter into two fields which become our pump and probe fields. A laser tuned to the D2 Rb is used as our repump field. The repump field is linearly polarized. The probe field is subjected to an Electro Optical Modulator (EOM) controlled by an radio frequency (RF) source generator. The pump field is produced by sending the D1 laser to an Acousto Optic Modulator (AOM),. The AOM modulated field is used as our pump in the experiment after being linearly polarized.

Our cavity consists of 4 mirrors arranged at  $45^\circ$  angles so that the reflected beams form a square. The cavity path contains a lens, 2 polarizing beamsplitters, and a Rubidium-87 cell. One of the mirrors is weighted and mounted on a Piezo Electric device (PZT).

The probe field is injected into the cavity. The probe passes through three mode matching lens elements before being injected into the cavity. The polarization of the probe field is such that the probe is transmitted through the beam splitters and continues to propagate

within the cavity, passing through the Rb cell with every trip. The pump field is passed through a single mode fiber optic cable before being combined with the repump field outside the cavity. The pump and repump are introduced into the cavity through one of the polarizing beam splitters. The combined pump and repump are reflected off of the PZT mirror into the Rb cell and then out of the cavity via another polarizing beam splitter. The pump and repump do not propagate within the cavity, as they are only allowed to pass through the Rb cell before being reflected outside the cavity due to their polarization. A small amount of the probe field is reflected outside the cavity by one of the polarizing beam splitters. The reflected probe field falls upon a photodiode (PD) and is analyzed by an oscilloscope, a spectrum analyzer, and sometimes with a lock-in amplifier.



**Figure 7** Picture of setup (red line is laser)

## Experimental Details

### *PZT Element and Lock-in Amplifier*

One of the mirrors inside the cavity was mounted on a weighted Piezoelectric element (PZT) (figure 8). PZT materials change their dimensions when an electric potential is applied. In the experiment, the PZT increased or decreased in length by a few micrometers based on the electric potential we set. The purpose of this modification was to simulate the rotation of the cavity by increasing and decreasing the cavity's path length by rapidly oscillating the potential applied to the PZT.

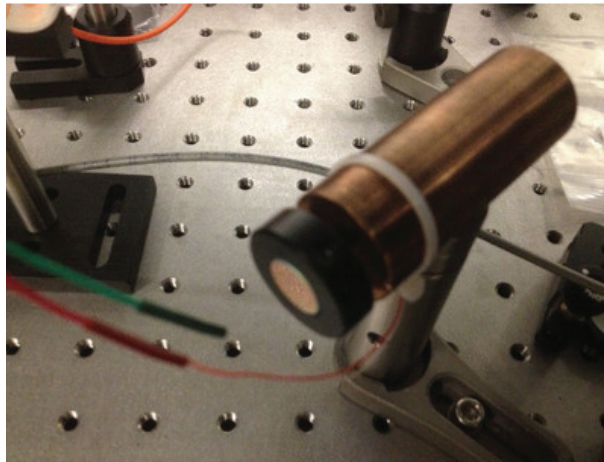


**Figure 8** Mirror mounted on PZT

The PZT also played a role in the stabilization of the cavity. Because the experiment relied on very precise spatial measurements, we wanted to be able to ignore small physical changes or oscillations in the cavity (like say from the instability of the table, changes in airflow due to noise or air currents, vibrations of mirrors, etc). To that end we set up the PZT in a feedback configuration with a lock-in amplifier. A lock-in amplifier is an electronic device that reads electrical inputs and locks on to their phase, frequency, and amplitude while ignoring background noise. To lock the probe laser onto our cavity resonance, we hooked the output of the amplifier to the PZT, so that when we were trying to stay on resonance the

amplifier would provide feedback to the PZT to slightly correct the path length of our cavity so that we could indefinitely stay on resonance, regardless of small fluctuations in the cavity.

### *D1 Field Modulation*

The probe field was produced using phase-modulation in an Electro Optical Modulator before being injected into the cavity. An EOM works by sending an RF electric field through a nonlinear optical material to modulate its index of refractive. We sent an RF signal at 6.915 GHz into the EOM to drive the modulation. The phase modulation causes the beam to develop many new harmonic frequency components every 6.915 GHz frequency difference from the original beam. The +1 and -1 sidebands are used in our experiment (fig 9). The sidebands differ from the original frequency by an amount equal to the RF signal frequency (6.915 GHz). The energy in both the sidebands is equal to the energy lost by the central band (conservation of energy), and in our experiment the sidebands contained about 40% of the total power each and the central band contained 20%. The sidebands physically overlap with the original beam, but only the bottom sideband (and not the top or central) is coupled into the cavity.

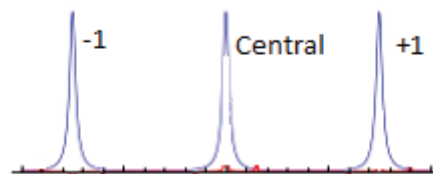


**Figure 9** Arbitrary laser central and sideband fields after EOM

The pump field was modulated by an Acousto Optic Modulator as opposed to an EOM. The modulation process is similar to that of the EOM, except the AOM uses acoustic waves

instead of electrical signals to modulate the refractive index of a crystal, which results in optical field modulation. The field generated by the AOM is physically separated at a given angle from the unmodulated field, unlike with the EOM. The new field has a frequency of - 80 MHz compared to the unmodulated field at the -1 order of diffraction, and we use the new field as our pump in the experiment.

### *Cavity Alignment, Assembly, and Optical Elements*

The cavity itself forms a square that is 77 cm in perimeter. The mirrors are specially coated so that they have 99.5% reflectivity for light wavelengths between 700 and 900 nm. The 30 cm focal length convex lens inside the cavity compensates for our cavity having flat mirrors instead of concave ones. The mirrors and external and internal lenses were aligned so that the beam would overlap with itself on many trips around the cavity.

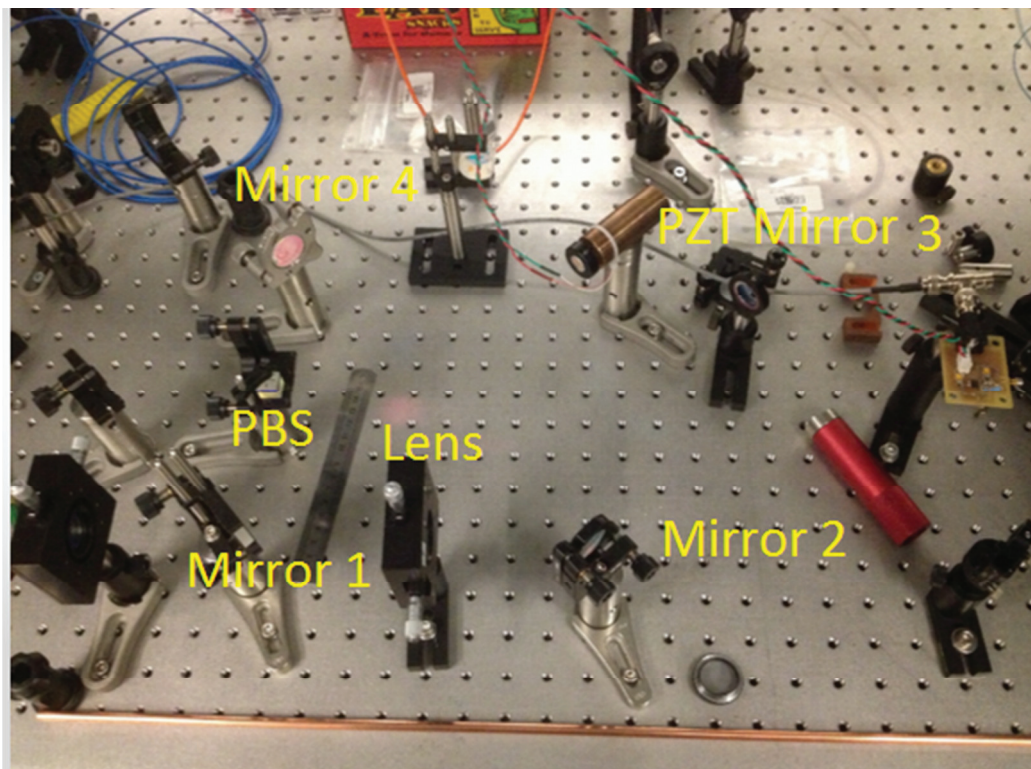


**Figure 10** “Empty” cavity during construction

The beam splitters are aligned with field polarizations such that the probe field is always transmitted and the pump and repump are always reflected while on the path the mirrors dictate. A flip mirror was placed in the path of the beam so that when the mirror was down the cavity behaved as normal and when the mirror was up we could observe the atomic interactions of the Rb cell with the pump and repump independent of the cavity setup.

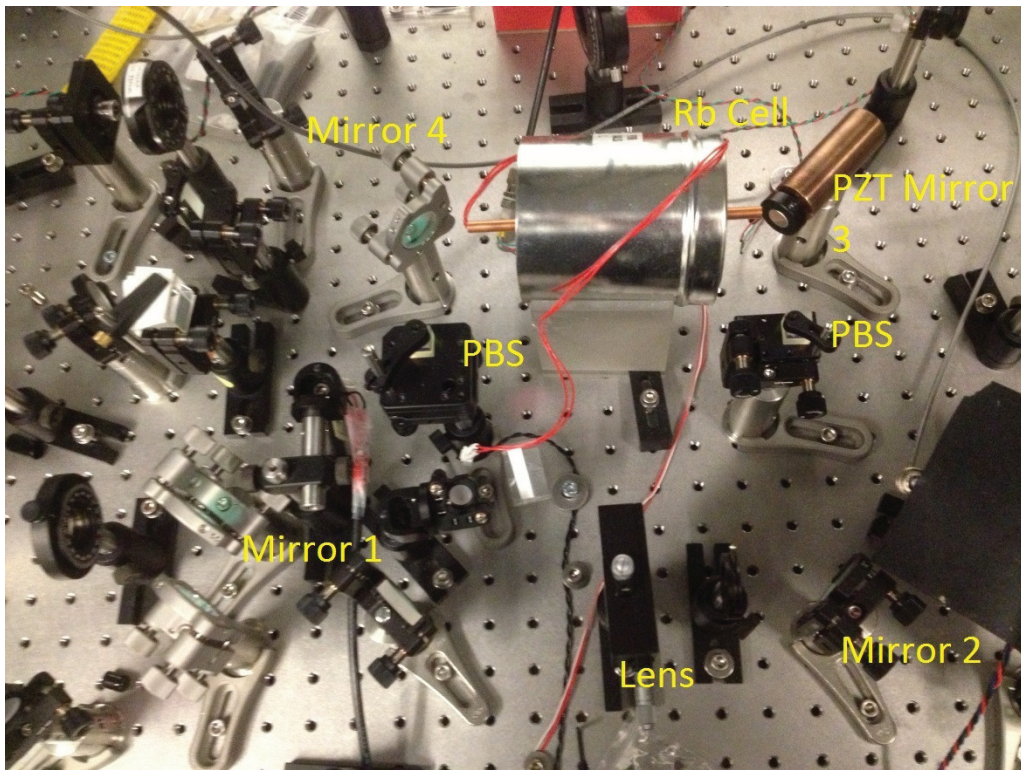


**Figure 11** Cavity during experiment

### *Laser Modes*

It was necessary for the probe field in the experiment to be in the  $TEM_{00}$  spatial mode. This mode corresponds to a Gaussian beam distribution, characterized by strong intensity in the beam's center and low intensity near the beam's edge (figure 12).

### Before Mode Matching



### After Mode Matching

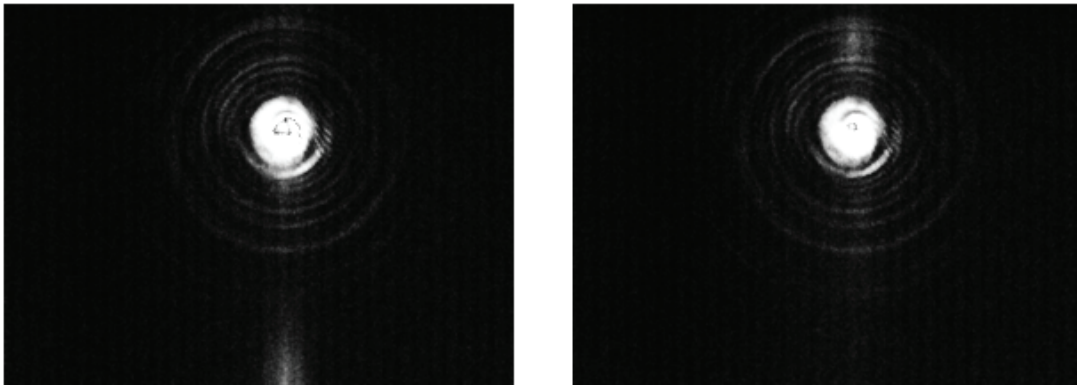


**Figure 12** Beam modes before and after mode matching

The interior and exterior spatial profiles of the cavity were numerically analyzed via a computer program so that they matched, and our computations determined that we needed to add 3 lenses outside the cavity and one inside the cavity to give us the desired low order mode. Before mode matching, our measurements determined that each mode resonated within the cavity, making it difficult or impossible to get useful data (figure 13).

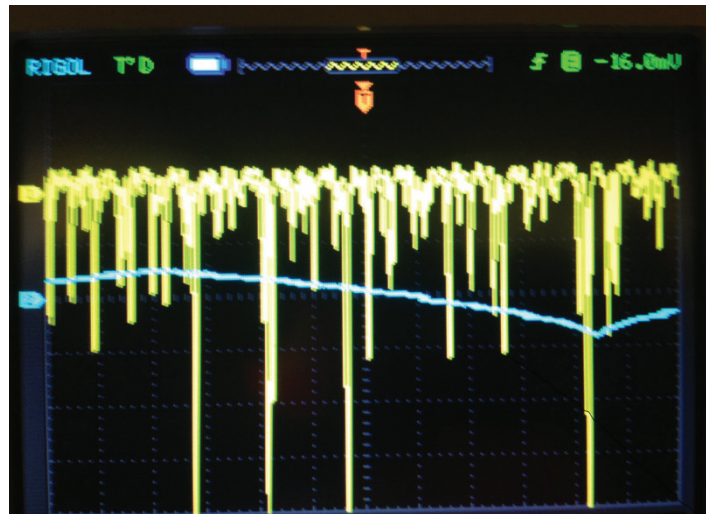


**Figure 13** Inverted cavity resonances before mode matching (in yellow)

After mode matching we saw only one mode, and a highly sensitive camera showed that it was the  $TEM_{00}$  mode, as desired (figure 14).

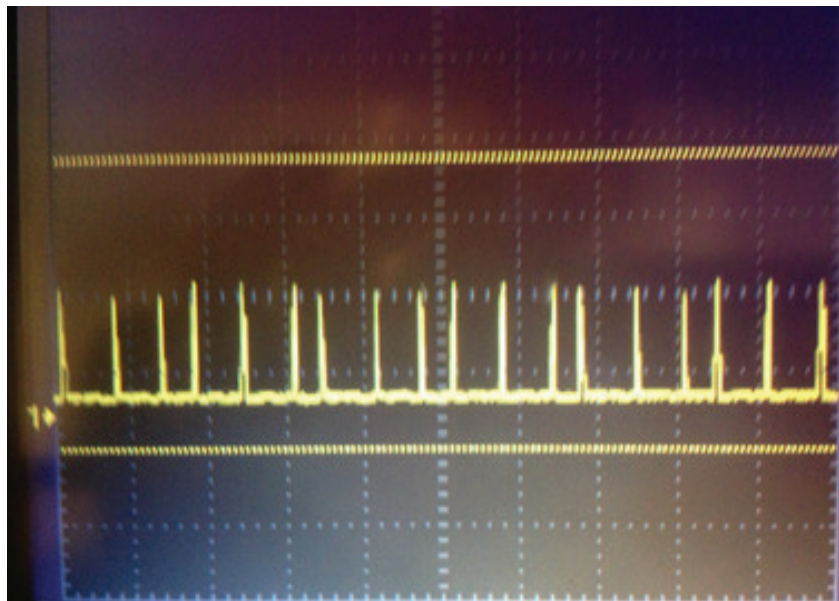


**Figure 14** Cavity resonances after mode matching (in yellow)

## *<sup>87</sup>Rb Cell*

The <sup>87</sup>Rb cell was encased in 3 layers of magnetically shielding material (figure 15). The cell was 25 mm long, 22 mm in diameter, pressurized to 5 Torr with Ne buffer gas, and heated to 90<sup>0</sup> C. The temperature was kept constant by active feedback. The temperature sensor was connected to the exterior of the cell, and set in feedback configuration with a temperature controller that maintained constant temperature by controlling the power applied to the heating wire wrapped around an inner layer of shielding.

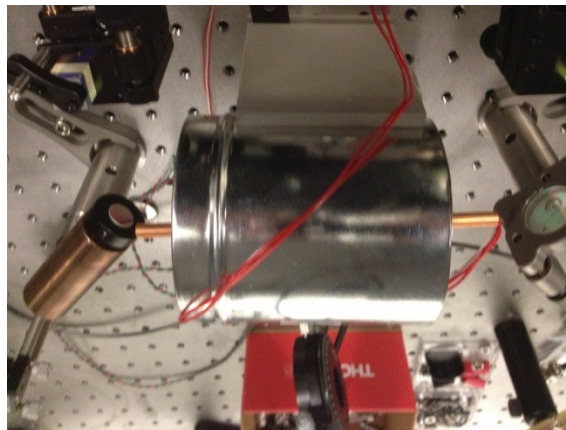


**Figure 15** Encased <sup>87</sup>Rb Cell

## *Optical Fields*

The probe and pump fields were tuned to the D1 line of <sup>87</sup>Rb at 795 nm. The repump field was tuned to the D2 line of <sup>87</sup>Rb at 780 nm. As mentioned in the Theory section of this document, we tuned the probe field to the F=2 to F'=1 or F'=2 transition in the D1 line, the pump field to the F=1 to F'=1 or F'=2 transition in the D1 line, and the repump field to the F=2 to F'=1, 2, or 3 transition in the D2 line. When determining parameters in the experiment, we swept the D1 and D2 lasers, scanning their frequencies with electronic control boxes and decreasing the scan as we approached our desired frequency.

When scanning frequency we often used the absorption of a Rubidium reference cell to gain our bearings, looking for noteworthy spectral structures to use as points of reference (figure

16). As we swept the laser frequency we were able to observe absorption lines at given frequencies and use known absorption spectra to determine what frequency the laser was at.

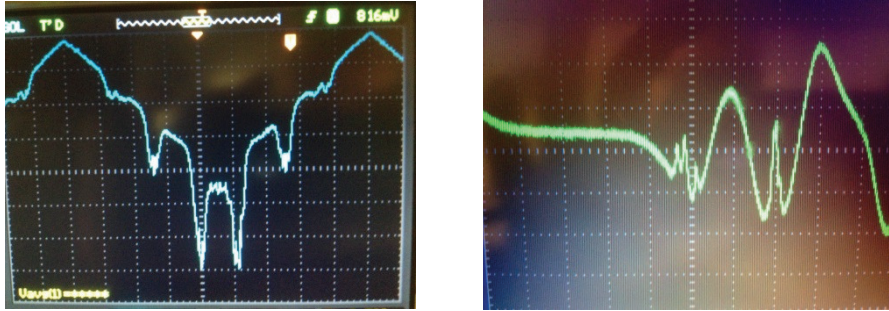


**Figure 16** D1(left) and D2 (right) saturation spectroscopy data

The above saturation spectroscopy figures resulted from a monochromatic laser shone through our Rb cell.

### *Measurements*

The beatnote of two fields is the wave packet created when the two fields periodically interfere constructively and destructively with each other. Measurements of the beatnote between the probe and pump fields were made on a spectrum analyzer connected to a fast photodiode (the photodiode had a fast response time for incoming signals). In the experiment we observed the beat note generated by the pump and the generated fields. Transmission measurements of the generated and probe fields through the cavity were made by a photodetector hooked up to an oscilloscope.

## Results and Analysis

### *Cavity Performance*

After assembling the cavity, we confirmed that it was transmitting the probe laser without the presence of the pump or repump fields while using the PZT to sweep cavity path length. We were able to adjust the mirrors such that by small variations in the laser's path we could observe smooth transitions onto cavity resonance conditions.

### *EIT*

After observing the cavity's optical resonance, we added the pump field to the setup and used the flip mirror to observe a single pass transmission of the probe and pump within the cavity. When the pump laser was tuned off resonance, we observed no transmission within the absorption line, as expected. As we tuned the pump field towards resonance conditions and changed the 2-photon detuning through the RF source driving the EOM, we observed transmission characteristic of a single  $\Lambda$  system in an EIT state. Our transmission peak was asymmetric because the pump and probe fields were detuned away from exact optical transitions.

In a later trial, we observed EIT conditions within the cavity with the flip mirror down. The resonance peaks in our cavity showed greater magnitude as the pump laser was tuned towards resonance conditions, consistent with our earlier findings.

### *Probe Field Generation Through Four Wave Mixing*

After adding the repump to our single  $\Lambda$  scheme, we observed probe generation consistent with Four Wave Mixing in a double  $\Lambda$  scheme. When observing the pump and repump

interaction with the  $^{87}\text{Rb}$  cell outside the cavity via flip mirror, we saw a strong symmetric peak with over 50% gain. We then swept our 2-photon detuning to find optimal detuning. A 2-photon detuning value of 6.83468 GHz gave us the largest transmission (figure 17a).

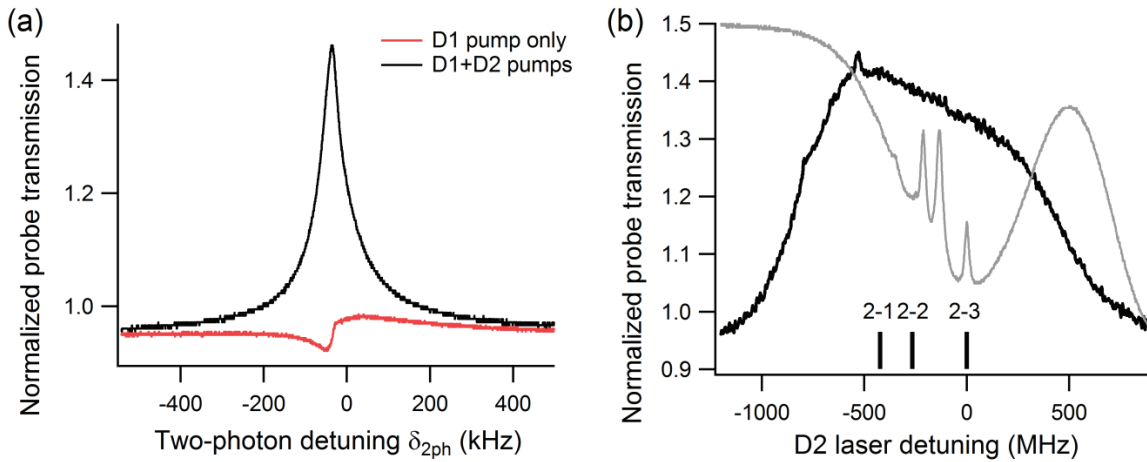


**Figure 17 a)** Probe transmission when repump is on and off and as detuning is scanned **b)** Probe transmission as repump laser is scanned

We then scanned our repump laser through the D2 line and observed the resulting amplified field to determine optimal detuning (figure 17b).

We allowed the probe field to circulate inside the cavity and observed the effect of the pump and the repump on the resonance peaks of the cavity. We observed high gain in the probe's transmission at resonance peaks, similar to the gain described above but to a greater extent (figure18).

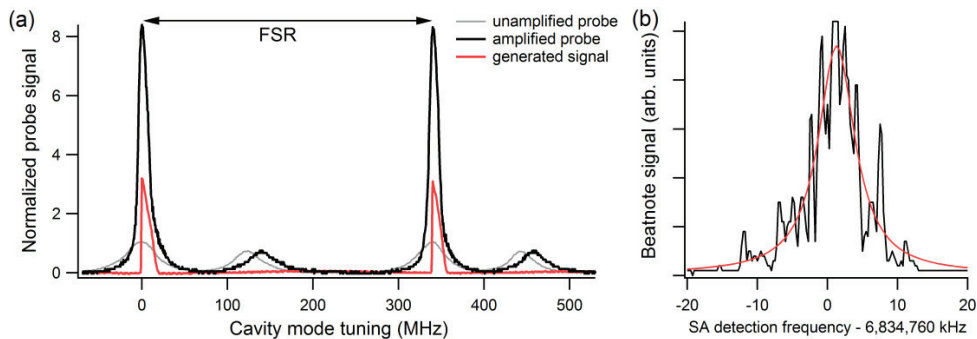


**Fig18 a)** Probe transmission as cavity is swept with PZT **b)** Beatnote of pump and probe fields on spectrum analyzer

We also varied the power of the pump and repump lasers independently to determine how lower beam intensity affected our scheme (figure 19). We observed a threshold power in the repump laser below which we did not observe generation at ~1 mW. At powers far above the threshold, we observed a drop off in rate of return for the amplitude of the generation. As we increased the repump power, a second spatial mode was generated. The second field was dependent on the alignment of the cavity and had much higher threshold values. When we increased pump power, the amplitude of the generation grew more or less linearly. This is not particularly surprising, as the range over which we could vary pump power was much smaller than that of the repump range.

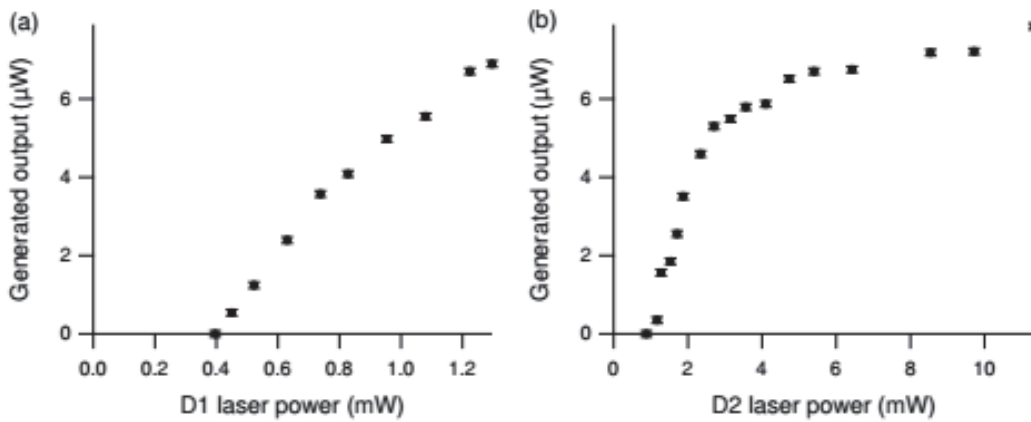


**Figure 19** Probe generated as pump **(a)** and repump **(b)** laser powers are varied. In part a) repump is set to 5.4 mW and part b) pump is set to 1.3 mW

The beatnote of the pump and probe laser was analyzed on the spectrum analyzer when the 2-photon detuning was set to 6.83471 GHz (figure 18b). The analysis of the beatnote confirmed that our generated field was at the probe frequency needed for the experiment.

## *Probe Delay and Advancement*

For this section of the experiment in which we examine advancement or delay of our probe field, we used Amplitude Modulation (AM) from our RF source to modulate the probe field.

The amplitude of our probe was modulated by a relatively small sine wave from the RF source at 12.5 KHz. The relatively small modulation amplitude allowed us to lock on to the cavity resonances with a lock-in amplifier without having to worry about the modulation interfering with the lock.

In the experiment we turned the pump and probe fields on, but the repump power was set just below the generation threshold. We used the RF source to sinusoidally modulate the amplitude of the probe laser by about 10% of the maximum probe amplitude at 12.5 KHz.

We stopped sweeping the cavity path length and used the PZT lock-in amplifier to lock on to a resonant transmission peak. The amplitude modulation was small enough that it did not interfere with the lock. Our control delay value was taken by blocking both pump fields and shifting the probe field's frequency far away from any atomic resonances.

We varied 2-photon detuning and observed the delay or advancement of the sinusoidal probe field relative to our control over a range of frequencies (figure 20). For detunings that gave us a maximum amplitude amplification, we observed delay characteristics of slow light. However, as we decreased our detuning we observed probe advancement characteristic of fast light.

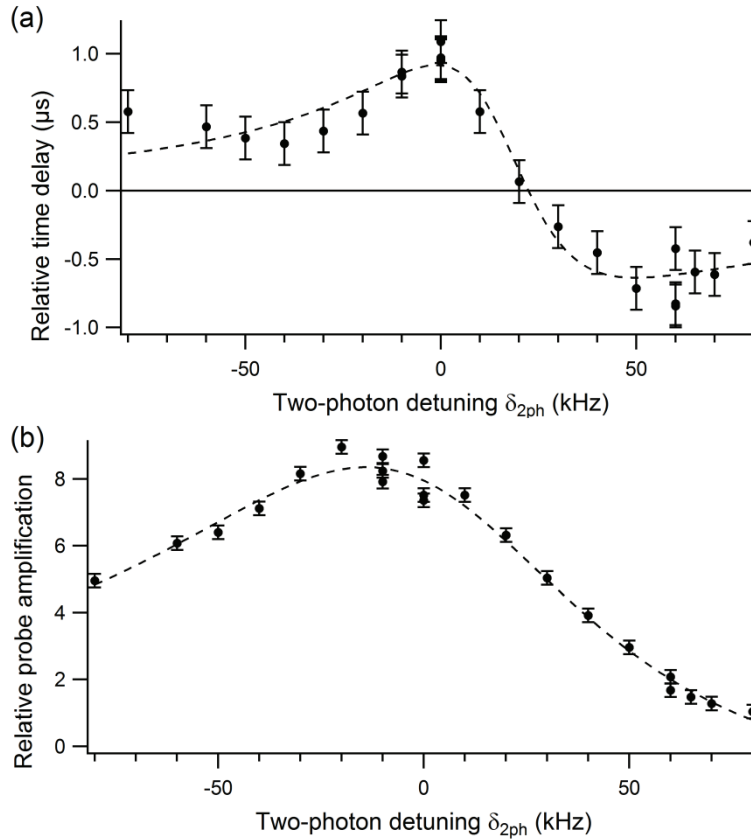


**Fig20 a)** Probe advancement as 2-photon detuning is varied **b)** Probe transmission for same detunings as in a)

### *Cavity Pulling*

We tested the capabilities of the cavity by observing how the frequency of the generated field changed as we swept cavity length. We used the same setup as for when testing the FWM capabilities in the cavity, except we also coupled a +1 sideband of the probe detuned by about 150 MHz into the cavity. The sideband was far away enough from resonance frequencies that it did not interfere with the probe field generation, yet it allowed us to lock the cavity and observe the frequency of the probe field shifting as the cavity was swept (figure 21).

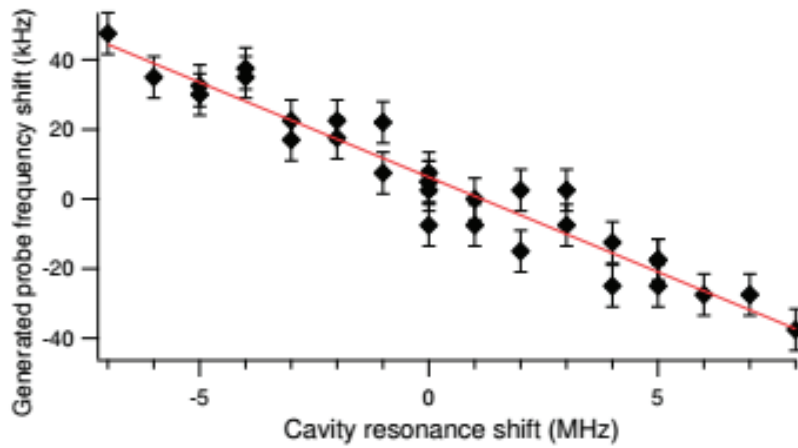


**Figure 21** Generated Probe frequency shift as resonance frequency of the cavity is changed

While the process itself was effective and produced reliable data, the parameters of the cavity prevent the system from being useful in precise measurements at this point. The finesse of the cavity needs to be an order of magnitude higher or the range of frequencies over which the FWM generation occurs needs to be much broader to allow the system to be viable in a gyroscope.

## Conclusions

We successfully constructed and tested a cavity that could eventually be used in a laser gyroscope. Using a  $^{87}\text{Rb}$  cell and a four level N-scheme, we successfully observed EIT, slow light, fast light, and four wave mixing in the cavity. The generation of the probe field in the cavity was very promising. However, the cavity needs to have a higher finesse or the FWM gain needs to be spectrally broadened in order to be used to test gyroscopic enhancement. It is also possible that the optical elements in the cavity could be better optimized for better results.

## **Acknowledgments**

I would like to thank Irina Novikova and Eugeniya Mikhailov for all the guidance they have provided over the last 2 years and Gleb Romanov for his counsel and his mystical fiber-optical alignment techniques. I would also like to thank the College of William and Mary for and the Naval Air Warfare Center for supporting our group's research.

## References

- [1] M. S. Shahriar, G. S. Pati, R. Tripathi, V. Gopal, M. Messall, and K. Salit, "Ultra-high enhancement in absolute and relative rotation sensing using fast and slow light," *Phys. Rev. A* 75, 053807 (2007).
- [2] Nathaniel B. Phillips, Irina Novikova, Eugeny E. Mikhailov, Dmitry Budker, Simon Rochester, "Controllable steep dispersion with gain in a four-level N-scheme with four-wave mixing," *Journal of Modern Optics* 60, 66-72 (2013).
- [3] E. Mikhailov, J. Evans, D. Budker, S. Rochester, I. Novikova, "Experimental studies of four-wave mixing in a ring cavity" (2014).
- [4] I. Novikova, E. Mikhailov, L. Stagg, S. Rochester, D. Budker, "Tuneable lossless slow and fast light in a four-level N-system"
- [5] B. E. A. Saleh, M. C. Teich, "Fundamentals of Photonics", John and Wiley Sons Inc. (1991).
- [6] R. W. Boyd, "Nonlinear Optics", 2nd Ed. Academic Press, (2003).
- [7] Matsko A.B., Kocharovskaya O., Rostovtsev Y., Welch G.R., Zibrov A.S., Scully M.O., "Slow, ultraslow, stored, and frozen light", *Advances in Atomic, Molecular, and Optical Physics*, Vol 46, 191-242, (2001).
- [8] D. C. Hutchings *et al.*, "Kramers–Kronig relations in nonlinear optics", *Opt. Quantum Electron.* 24, 1 (1992).
- [9] E. E. Mikhailov, V. A. Sautenkov, I. Novikova, and G. R. Welch, "Large negative and positive delay of optical pulses in coherently prepared dense Rb vapor with buffer gas," *Phys. Rev. A* 69(6), 063808 (2004).

